Planetary transit candidates in the CoRoT SRa01 and SRa02 fields

J. Weingrill[1], S. Aigrain[2], F. Bouchy[3,4], M. Deleuil[5], C. Moutou[5], R. Alonso[5], P. Barge[5], A. Bonomo[5], P. Bordé[6], J. Cabrera[7], L. Carone[8], St. Carpano[9], D. Ciardi[10], Sz. Csizmadia[7], H. Deeg[11], R. Díaz[3,4], St. Dreizler[12], R. Dvorak[13], A. Erikson[7], F. Favata[9], S. Ferraz-Mello[14], E. Flaccomio[15], M. Fridlund[9], D. Gandolfi[9], N. Gibson[2], M. Gillon[16], E. W. Guenther[17], T. Guillot[18], A. Hatzes[17], G. Hébrard[19,5], L. Jorda[5], H. Lammer[1], A. Léger[6], A. Llebaria[5], C. Lovis[19], T. Mazeh[20], A. McQuillan[2], L. Nortman[12], A. Ofir[21], M. Ollivier[6], M. Pätzold[8], D. Queloz[19], H. Rauer[7], D. Rouan[16], B. Samuel[6], A. Santerne[5], J. Schneider[22], G. Wuchterl[17], K. Zwintz[13]

J. Weingrill, S. Aigrain, F. Bouchy, M. Deleuil, C. Moutou, R. Alonso, P. Barge, A. Bonomo, P. Bordé, J. Cabrera, L. Carone, St. Carpano, D. Ciardi, Sz. Csizmadia, H. Deeg, R. Díaz, St. Dreizler, R. Dvorak, A. Erikson, F. Favata, S. Ferraz-Mello, E. Flaccomio, M. Fridlund, D. Gandolfi, N. Gibson, M. Gillon, E. W. Guenther, T. Guillot, A. Hatzes, G. Hébrard, L. Jorda, H. Lammer, A. Léger, A. Llebaria, C. Lovis, T. Mazeh, A. McQuillan, L. Nortman, A. Ofir, M. Ollivier, M. Pätzold, D. Queloz, H. Rauer, D. Rouan, B. Samuel, A. Santerne, J. Schneider, G. Wuchterl, K. Zwintz

[1]Space Research Institute/ÖAW, 8042 Graz, Austria

[2]Oxford Astrophysics, Denys Wilkinson Building, UK

[3]Institut d'Astrophysique de Paris, 75014 Paris, France

[4]Observatoire de Haute Provence, France

[5]Laboratoire d'Astrophysique de Marseille, France

[6]Institut d'Astrophysique Spatiale, Université Paris XI, France

[7]Institute of Planetary Research, German Aerospace Center, Berlin, Germany

[8]Rheinisches Institut für Umweltforschung an der Universität zu Köln, Germany

[9]Space Science Department, ESA, Noordwijk, Netherlands

[10]Department of Astronomy, 211 Space Sciences Building, University of Florida, Gainesville, FL 32611, US

[11]Instituto de Astrofísica de Canarias, E-38205 La Laguna, Tenerife, Spain

[12]Institut für Astrophysik, Universität Göttingen, Germany

[13]University of Vienna, Institute of Astronomy, Austria

[14]Universidade de Sao Paulo/ Instituto de Astronomia Geofisica e Ciencias Atmosfericas, Sao Paulo, Brasil

[15]Palermo Observatory, Palermo, Italy

[16]LESIA, Observatoire de Paris-Meudon, France

[17]Thüringer Landessternwarte, Tautenburg, Germany

[18]Institut d'Astrophysique et de Géophysique, Université de Liège, Belgium

[19]Observatoire de l'Université de Genève, Switzerland

[20]Wise Observatory, Tel Aviv University, Tel Aviv 69978, Israel

[21]School of Physics and Astronomy, Tel Aviv University, Israel

[22]LUTH, Observatoire de Paris, CNRS, Université Paris, France

Abstract CoRoT is a pioneer space mission to detect stellar oscillations and transiting exoplanets. Large stellar fields are observed in runs up to 120 days to look for transit-signals. We present a list of detected transiting planetary candidates as well as eclipsing binaries as a by-product in the constellation Monoceros. 8190 targets were observed in the run SRa01 in March 2008 and 10300 targets in SRa02 in October 2008. 381 transiting objects were identified in both observation runs by different detection teams. Interesting candidates were additionally investigated with photometric- and radial velocity-observations. We present 11 possible planetary candidates in the constellation Monoceros in the short run SRa01 with one Saturn-like object still to be investigated and 19 possible candidates in the short run SRa02, one of them confirmed as a brown dwarf.

Keywords Techniques: photometric — Stars: planetary systems — binaries: eclipsing

1 Introduction

The CoRoT space mission is devoted to the observation of stellar variability and oscillations and to detect transiting extrasolar planets down to several Earth masses (Baglin et al. 2006). The mission has been extented until March 2013 due to its success. CoRoT has been observing more than hundred thousand targets in the galactic center and anti-center direction since the beginning of the mission. Its field of view is $2^\circ \times 2^\circ$ in a zone of ten degrees diameter. SRa01 and SRa02 were the first two short runs of the mission, which lasted around 25 days. Both runs described in this paper have been observed in the constellation Monoceros. For brighter stars color information is available, targets fainter than approximately 15 magnitudes are measured in white light only. These light curves have a cadence of

512 seconds, interesting targets have a shorter cadence of 32 seconds to ensure a precise transit timing. In the first stages of the data processing pipeline, invalid data-points caused by cosmic ray hits, obvious hot pixels and other alterations caused by the crossing of the CoRoT satellite through the Southern Atlantic Anomaly are flagged.

The data from SRa01 and SRa02 have been released to the public in March 2010 and May 2010 respectively, and are available through the Exo-Dat archive[1] (Deleuil et al. 2009). In this paper we present 11 possible planetary candidates for the short run SRa01 and 19 candidates for SRa02 as well as a list of eclipsing binaries (EB) for both.

The description of the detection process and the list of planetary candidates with their most important properties is given in Sect. 3. We will give an overview from the photometric and radial-velocity follow-up for each candidate in Sect. 4 and a detailed discussion and analysis in Sect. 5.

The primary target of SRa01 was the young ($\sim$ 3 Myr) open cluster NGC 2264 (Sung et al. 2004), which is the richest open cluster observable by CoRoT. The main additional science goals of the observations were to study rotation and activity (Favata et al. 2010), accretion processes (Alencar et al. 2010; Flaccomio et al. 2010) and pre-main sequence pulsations (Zwintz et al. 2011), and to search for eclipsing binaries in order to calibrate stellar evolution models.

This paper reports on the search for planetary transits and eclipsing binaries, but covers only the follow-up of the candidate transits. A more detailed analysis of a subset of the eclipsing binaries, which were suspected members of NGC 2264, will be presented in a forthcoming paper.

2 CoRoT observations

CoRoT observations of the SRa01 field started on March 3rd 2008 and lasted 24 days. The corners of the exoplanet field were located at: $6^h44^m57^s$ $10°21'16''$, $6^h50^m15^s$ $10°23'01''$, $6^h50^m20^s$ $7°42'07'''$, $6^h44^m57^s$ $7°41'34''$. Thus, the entire cluster was placed on CCD E1 (one of the two exoplanet CCDs). During that period, 8 190 stars were observed in the exoplanet channel, approximately 1 700 of which were previously known or candidate members of NGC 2264. Almost all the stars fall within the usual magnitude range $11 < R < 16$ for the CoRoT exoplanet channel. A handful of pre-main sequence B stars belonging to NGC 2264, with $9.2 < R < 11$, were observed despite being saturated, in order to search for pulsations (see Zwintz et al. 2011).

CoRoT observations of the SRa02 field started on October 11rd 2008 and lasted 32 days. The corners of the exoplanet field were located at: $18^h30^m20^s$ $7°36'42"$, $18^h31^m08^s$ $7°13'54"$, $18^h39^m20^s$ $5°02'30"$, $18^h34^m11^s$ $4°41'30"$. During that period, 10 305 stars with magnitudes $11 < R < 16$ were observed in the exoplanet channel. The planetary nebula PN G204.8-03.5 has been observed as the target E2_2404 and members of the open cluster NGC 2236 in the field of the CCD E1. There are other sources that had been observed like E1_2883, which is identical with the infrared source IRAS 06269+0625 or E2_4632 that points to the radio source 4C +04:23.

The light curves were produced using the CoRoT pipeline (Auvergne et al. 2009) and are publically available from the CoRoT archive at IAS[2].

The noise statistics of both short runs are pretty consistent with the first run IRa01 (Aigrain et al. 2009). The RMS scatter of the SRa01 light curves is somewhat larger, at a given magnitude, than for other CoRoT short runs (see Fig. 1). This is partially due to the fact that a significant fraction of the target stars are young and thus active and/or accreting. The field is also closer to the edge of the CoRoT continuous viewing zone in the Galactic anticentre, and consequently suffers from slightly increased jitter and scattered light contamination.

3 Transit candidates

3.1 Transit and eclipse detection

During most CoRoT observations, a near real-time analysis (known as the 'alarm mode') is performed during the run on partially calibrated data, in order to identify potentially interesting events and trigger oversampled observations for the corresponding targets (32s rather than the usual 512s sampling). The majority of the highly significant transit-like events are usually detected at this early stage.

For SRa01, no alarm mode analysis was performed. Therefore all the candidates were identified from the fully calibrated, complete light curves. A total of 6 teams (based at DLR, ESTEC, Exeter, IAS, Köln and LUTH) searched the light curves for transit-like events, using a range of detrending and transit detection algorithms, and assigned a preliminary ranking to each candidate: priority 1, 2 and 3 for possible planetary

[1] http://lamwws.oamp.fr/exodat/

[2] http://idoc-corotn2-public.ias.u-psud.fr/

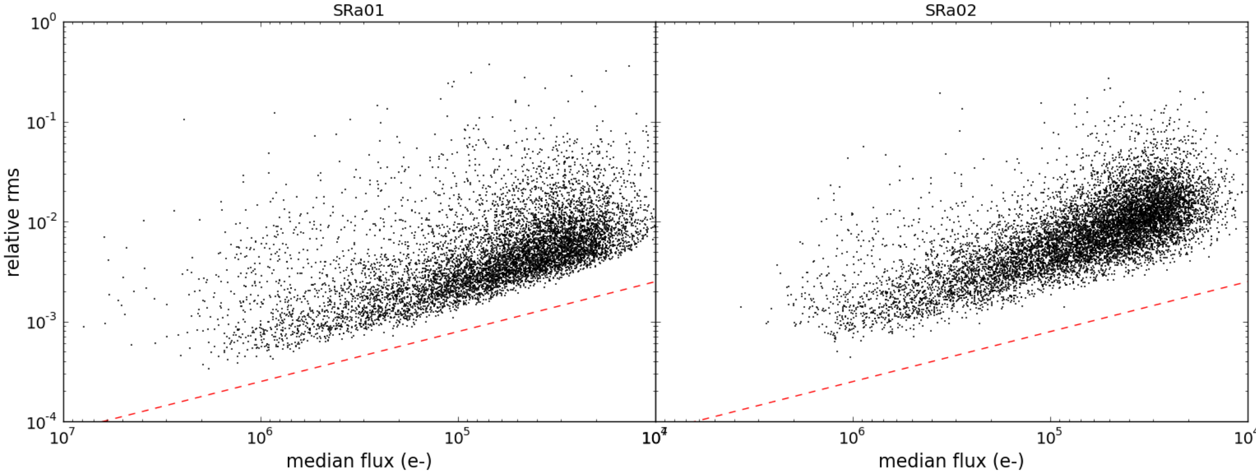

Fig. 1 The relative RMS as a function of median flux in the light curve for both runs, with the source photon noise as the red dashed line.

transits, and 'B' for clearly stellar EBs. The candidate lists produced by individual teams were merged automatically, resulting in a total of 163 events.

For SRa02, 5 candidates were identified from the alarm mode analysis. Further transit searches were run on the fully calibrated, complete light curves by 3 teams (based at DLR, ESTEC and Köln), resulting in a total of 218 candidate transits and likely EBs, with associated preliminary rankings. Additional candidates came from the SARS algorithm by Ofir et al. (2010), which allows to search for even fainter transits.

3.2 Preliminary sifting of the candidates

Among the scenarios which, to first order, can mimic planetary transits, a large fraction can be identified from a detailed analysis of high-precision transit light curves only, before any follow-up is performed. A description of this process has been given in previous CoRoT run summary papers (Carpano et al. 2009, Carone et al. submitted), but we have recently adopted a more systematic approach, using automatically produced diagnostic plots and transit fits to assess the candidates. We therefore give a brief description of this procedure below.

Each candidate that was identified as a possible planet (rather than a definite EB) by at least one team was assessed individually, starting with visual examination of the individual transit-like events and of the phase-folded light curve. A number of candidates were identified as likely artefacts at this stage, caused by discontinuities in the light curves[3]. Transit-like events with depths exceeding 5% were automatically discarded as likely binaries. Events with depths between 2 and 5% are relatively unlikely to be of planetary origin, but a number of these, with precise light curves compatible with low impact parameter transits, were retained nonetheless: if the companion is a low-mass star or brown dwarf, it is relatively straight forward to identify from a small number of follow-up observations, and scientifically interesting in its own right.

For the remaining candidates, the transit-like events were modelled in the white light curves using the (Mandel and Agol 2002) formalism. The fits were optimized using the MPFIT implementation of the Levenberg-Markwart algorithm in Python. The parameters of the fits were the period P, the time of transit centre T_0, the planet-to-star radius ratio $R_\mathrm{p}/R_\star$, the impact parameter b and the system scale $a/R_\star$. We used a quadratic limb-darkening model with (fixed) parameters $u_a = 0.44$ and $u_b = 0.23$, which are suitable for a $0.9\,M_\odot$ main-sequence star in the CoRoT bandpass (Sing 2010). We used both the formal errors of the fit and residual shuffling (the 'rosary bead' method) to estimate the uncertainties in the fitted parameters (the two methods usually give near-identical results, the larger of the two uncertainties was adopted). The baseline level around each transit was modelled using a localised second-order polynomial fit, which accounts for long-term trends and stellar variability. We used an iterative process, alternately refining the transit shape on the folded light curve, then fitting the times of individual transits to refine the ephemeris, until convergence

[3]CoRoT crosses the Earth's radiation belts several times per day, making it particularly susceptible to charged particle impacts, which can cause individual pixels to behave erratically and lead to discontinuities in the light curves.

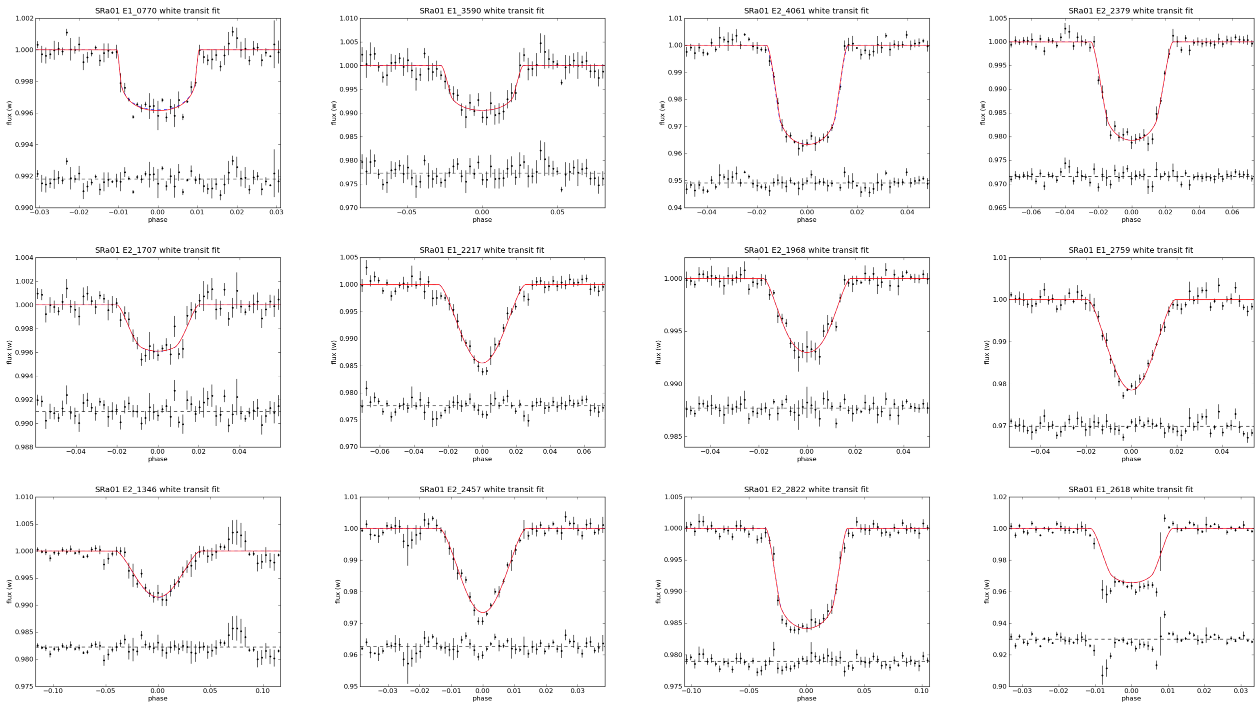

Fig. 2 Phase-folded light curves of the transit candidates for run SRa01, showing the best-fit transit model (red) and residuals in each case. The phased light curves have been binned to 20 points per transit duration for clarity.

was reached. Odd- and even-numbered transits were then fitted separately, varying the transit depth only, to test for signs of binarity. We also fit the blue, green and red light curves (when available), again varying the transit depth only. Finally, we performed a search for secondary eclipses with the same duration as the best-fit transit model, and checked for ellipsoidal variability by fitting the phase-folded out-of-transit light curves using a sum of sines and cosines at the transit frequency and its first harmonic.

The detection of secondary eclipses or differences in depth between odd- and even-numbered transits, or strong ($> \times 2$) differences in depth between the three colour channels, precludes a planetary origin for the transit, as does a transit shape and duration implying a stellar radius $> 3R_{\odot}$, or a transit depth $> 5\%$. Candidates were thus discarded as grazing or diluted eclipsing binaries (EBs) if these effects were detected at the $\geq 5\sigma$ level. The shape of the transits, as well as weaker detections of these effects or of ellipsoidal variations were used to rank the remaining candidates, but were not considered to exclude a possible planetary origin.

3.3 Final candidate and EB lists

12 transit candidates from run SRa01, and 19 from run SRa02, pass the tests described in the previous section. They are listed in Tables 1 and 2 respectively, and their light curves (along with the best-fit transit model) are shown in Figures 2 and 3. Since the final candidate list was drawn up, further refinements to the light curve modelling have led us to consider two of the priority 3 candidates in SRa01 as closed: E1_2618 is very likely to be a false alarm (caused by discontinuities in the light curve), whilst a re-analysis of the light curve of E2_2822 detected a secondary eclipse and ellipsoidal variation (both at the 5σ level), so it is likely to be a diluted EB.

Tables 3 and 4 lists the EBs identified as a side product of the transit detection and sifting process. These lists contain all detectable, well-detached systems, but are incomplete for near-contact or over-contact systems. Note that these tables merely report the output of the transit search process: no attempt has been made to check that the period identified is indeed the orbital period, to account for contamination of the aperture or to refine the eclipse depths.

4 Follow-up observations

Ground-based follow-up observations are necessary to confirm the planetary nature of transit candidates, since a wide range of astrophysical scenarios involving two or more stars can mimic a planetary transit. A general description of the scenarios that can mimic a planetary transit, and of the follow-up strategies used

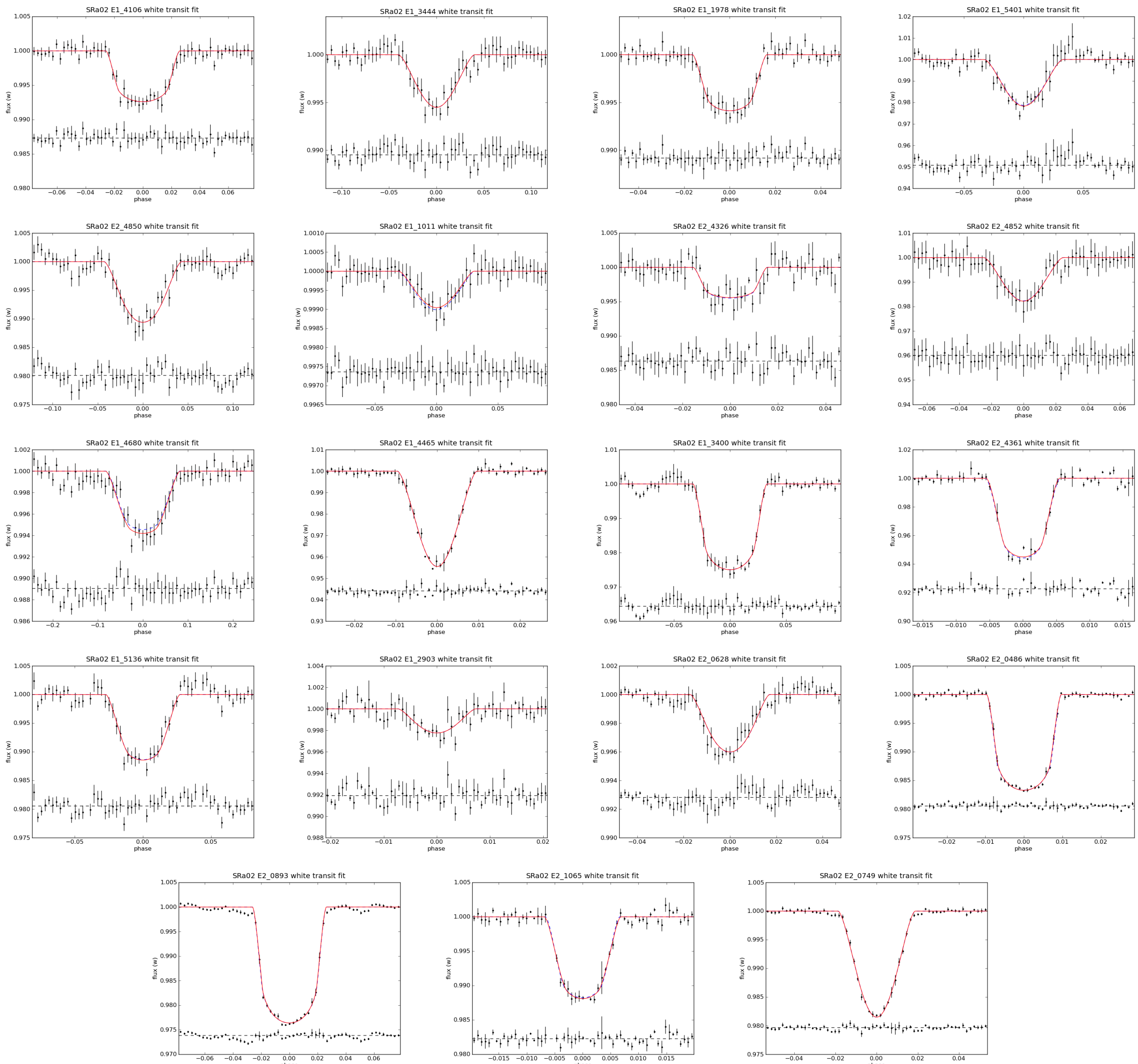

Fig. 3 Phase-folded light curves of the transit candidates for run SRa02. Same legend as Figure 2.

to discard them, is given in (Bouchy et al. 2009). The follow-up observation strategy for CoRoT candidates, first described in (Moutou et al. 2009), consists primarily of a) photometric observations in- and out-of-transit, with a larger telescope (typically 1 m), to test whether the object being eclipsed is the brightest star in the photometric aperture or a fainter star with a deeper eclipse (a 'blend'), and b) radial velocity (RV) observations to determine the companion mass and rejected undiluted binaries.

The follow-up prioritization (reported in Table 1) was based on the prioritisation emerging from the detection process, but also incorporated how factors which make precise RV determination more or less difficult, including the brightness of the star and its rotation period (where it could be determined from a Lomb-Scargle periodogram analysis of the out-of-transit light curve). Pressure on the telescope time available implied that only priority 1 and 2 candidates were actually observed.

4.1 Photometric follow-up

The photometric follow-up program, its motivation and its techniques are described in more detail in (Deeg et al. 2009). For the runs described here, most of the observations have been made with the following telescopes: the 1m at the Wise observatory in Israel, the 80 cm telescope of the Instituto de Astrofísica de Canarias (IAC) and the 3.6 m CFHT in Hawaii. The short duration of the SRa01 and SRa02 runs did not enable a very accurate determination of the period of the candidate transits. In consequence, after the end of the CoRoT observations, a rapid ground-based follow-up is required before timing errors become larger than a few hours, when such follow-up becomes unfeasable.

The follow-up of SRa01 candidates could however not start until the winter 2008/2009, as CoRoT observed this field in spring 2008 at the end of its visibility, and at the time the CoRoT data were processed and searched for transits it was no longer observable. In consequence, only four candidates were observed; with some of them with ambigous results due to uncertainties in the time of the transit events. In SRa02, the photometric follow-up could start shortly after the CoRoT-data were acquired; and a total of eight SRa02 condidates were observed.

4.2 Spectroscopy

Radial velocity (RV) observations of short run SRa01 and SRa02 were performed with the SOPHIE spectrograph (Perruchot et al. 2008; Bouchy et al. 2009) mounted at the 1.93-m Haute Provence Observatory (OHP) telescope (France) and with the HARPS spectrograph (Mayor et al. 2003) mounted at the 3.6-m ESO telescope (Chile) as part of the ESO large program 184.C-0639. SOPHIE and HARPS were both used with the observing mode obj_AB, without simultanenous thorium in order to monitor the Moon background light on the second fiber. The exposure time was usually set from 0.5 to 1 hour. We reduced SOPHIE and HARPS data and computed RVs with a pipeline based on cross-correlation techniques (Baranne et al. 1996; Pepe et al. 2002).

Given the weak ephemeris constraints and the absence of photometric follow-up for SRa01, only candidates with magnitude $R < 15$, where direct radial velocity follow-up would not be excessively costly, were observed in RV for this run, using the equivalent of 9 hours of telescope time on SOPHIE and 7 hours on HARPS were used to follow-up SRa01 candidates. The equivalent of 17 hours on SOPHIE and 15 hours on HARPS were used to follow-up SRa02 candiates.

5 Details of individual candidates

5.1 SRa01 candidates

SRa01_E1_0770: This candidate shows 0.4%-deep, U-shaped transits lasting 3.4 hours with a period of 6.7 days (see Figure 2). Marginal differences between the transit depths measured in the red and blue channels may indicate a crowded aperture, but do not exclude a grey transit on the main target. All other indicators being compatible with a planetary transit, this candidate was classified as priority 1 by the detection team, and put forward for follow-up with priority 1. The light curve also shows clear quasi-periodic modulation with a period of 10.4 days and a semi-amplitude of about 1% (see Figure 5), which we attribute to rotational modulation of star spots.

Six observations were conducted with SOPHIE between December 2008 and Februray 2009. The derived RVs show no significant variations at the level of the uncertainties, which are ~ 35 m s^{-1}. One Keck spectrum was acquired on the 5$^{\rm th}$ of December 2009 and the spectral analysis indicates a G2…G5 dwarf with $T_{\rm eff} = 5860^{+100}_{-180} K$ and $\log g = 4.2 \pm 0.20$. We also observed this candidate with HARPS in January and February 2010, obtaining seven RV measurements with uncertainties in the range 10…20 m s^{-1}at a signal-to-noise ratio of 190 at 5870 A , shown in Figure 4. These data are compatible with low-amplitude RV variation of $v \sin i = 5.0 \pm 1.5$ km s^{-1}in phase with the transits: the

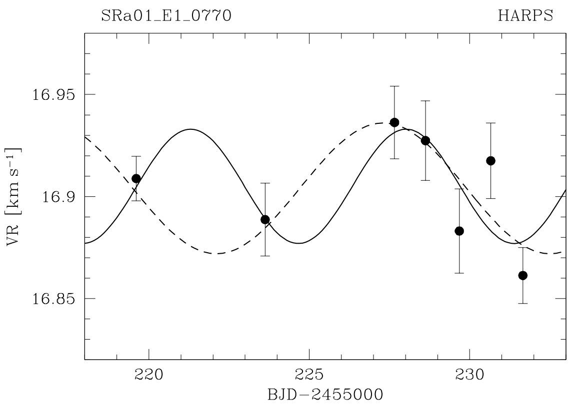

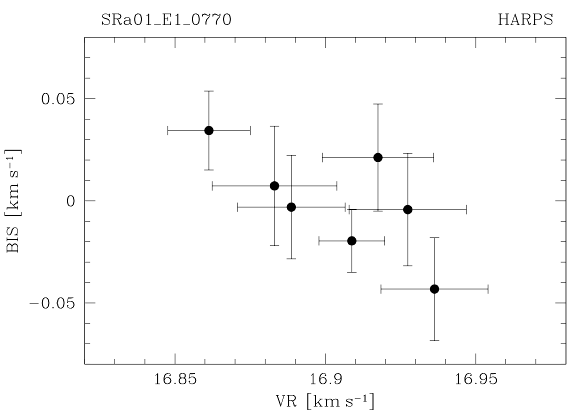

Fig. 4 (Top) HARPS RVs of SRa01_E1_0770, showing a hint of variation in phase with the transit ephemeris (solid curve) as well as with the stellar rotation period (dotted curve). (Bottom) Bisector span versus RV, showing an anti-correlation indicating that the RV variations are at least partially due to the stellar activity.

best sinusoidal fit to the RVs then has a semi-amplitude of $K = 28 \pm 10 \ \ \mathrm{m\,s^{-1}}$. However, an equally valid solution with similar amplitude is found at the stellar rotational period. The RVs appear to be anti-correlated with the line bisector span (see Figure 4, bottom panel), which suggests that at least some of the observed RV variation is due stellar activity. This fact is emphasized by a small emission feature in the CaIIK-line and variations in H_α. With our present data, we can exclude undiluted companions with a mass$> 0.6\,M_\mathrm{J}$, but we cannot firmly establish the nature of the transiting object. Assuming a Sun-like star with $1.057 \pm 0.07\mathrm{M}_\odot$, a companion would have to have a radius of $\sim 0.6\,R_\mathrm{J}$ to cause transits with a depth of 0.4%. If its density was similar to Jupiter's, it would have a mass of $\sim 0.2\,M_\mathrm{J}$, and induce RV variations in its host star with a semi-amplitude of $\sim 20\ \mathrm{m\,s^{-1}}$. A planetary scenario is thus still possible and supported by the Li I line feature, but additional RV measurements with higher precision and a good coverage of the stellar rotational cycle will be necessary to establish the true nature of this candidate. However, photometric follow-up is needed to confirm that the star being eclipsed is the main target, rather than a fainter background star, before an intensive RV campaign can be launched.

ON-OFF photometry was obtained on this candidate with the CFHT on 20 Nov 2009, leading to a tentative detection of an 0.3% deep transit on the target. The target is a well-isolated star; the closest neighbor visible in the CFHT imagery is a 3.1 mag fainter star 26 arcsec SW that does not generate any measurable contamination in the Corot aperture mask.

SRa01_E2_2379: This candidate shows 2.2%-deep U-shaped transits lasting 3.8 hours with a period of 3.6 days. The host star is and quite blue ($B-V = -0.1$, $J-K = 0.0$), indicating a moderately early-type field object confirming the suspicion from the broadband colours and transit duration. The light curve shows tentative signs of binarity (marginal depth differences between odd- and even-numbered transits, marginal detection of a secondary eclipse), which led to a priority 2 classification by the detection group. However, given the relative scarcity of high-priority candidates bright enough for spectroscopic follow-up in this run, this candidate was given priority 1 for follow-up observations. The determination of the P_rot of the host star is problematic as the detection of a modulation at 9.7 ± 1.2 days is very tentative. A shorter rotation period can be excluded.

A single HARPS exposure of this object was obtained in November 2009. Not peak was detected in the cross-correlation function (CCF), indicating an early type and/or very rapidly rotating star. Observations of this objects were therefore discontinued.

A transit on SRa01_E2_2379 was clearly seen on the target with a depth of 2% in CFHT follow-up observations on 19 Feb 2009.

SRa01_E1_2217: This candidate shows 2.7%-deep V-shaped transits lasting 2.8 hours with a period of 2.7 days. Together with the transit shape, marginal depth differences between odd- and even-numbered transits led to a priority 2 classification by the detection group, and the same priority was adopted for the follow-up.

E1_2217 was observed with SOPHIE in January 2009, the resulting RVs are shown in Figure 6. Although the uncertainties of the semi-amplitude are relatively large ($\sim 150\,\mathrm{m\,s^{-1}}$), the RV variations are not in phase with the CoRoT ephemeris. The amplitude of the variation is also dependent on the choice of template used to compute the CCF (results for F0, G2 and G5 templates are shown). This is the signature of a spectroscopic blend due to a diluted EB within the 3 arcsec acceptance diameter of the SOPHIE fibre, a result that was supported from photometric observations with the 3.5 m WIYN telescope in January 2010.

SRa01_E2_1707: This candidate shows 0.4%-deep U-shaped transits lasting 2.3 hours with a period of 2.4 days. The transit shape could not be determined conclusively from the relatively noisy light curve. Marginal depth differences between odd- and even-numbered transits led to a priority 2 classification by the detection group, and the same priority was adopted for the follow-up.

Three HARPS observations that were performed on 13, 14 and 15th February 2010 of this candidate, the resulting RVs are shown in Figure 7. No signification variation is detected the level of 28 $\mathrm{m\,s^{-1}}$. Assuming a Sun-like star, a companion would have to have a radius of $\sim 0.7\,R_\mathrm{J}$ to cause transits with a depth of 0.4%. If its density was similar to that of Jupiter, it would have a mass similar to that Saturn, and induce RV variations in its host star with a semi-amplitude of ~ 40 $\mathrm{m\,s^{-1}}$. Such a signal is excluded by the HARPS measurements. The remaining possibilities are thus a transiting sub-Saturn mass companion, or a blend with a close contaminant. The tentative detection of differences in depth between the odd- and even-numbered transits supports the latter scenario. The solar-like host-star has an effective temperature of $5600^{+120}_{-80}K$ and a $\log g$of $4.05^{+0.15}_{-0.30}$.

No preparatory or follow-up imagery of this target exists; an uncatalogued 19mag star 6” NW can be recognized in the POSS, which could be a potential source of a false positive.

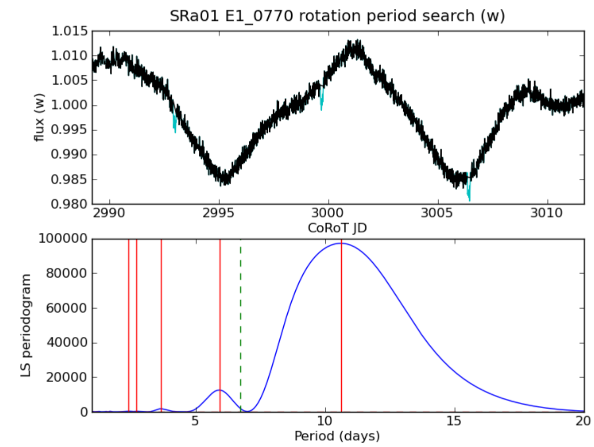

Fig. 5 Full light CoRoT curve for SRa01_E1_0770 (top, linear trend subtracted), and corresponding Lomb-Scargle periodogram (bottom), showing the clear detection of rotational modulation with a period of 10.4 days. The periodogram was computed after excluding the in-transit sections of the light curve (shown in blue in the top panel). In the bottom panel, the vertical solid red lines indicate the 5 most significant peaks in the periodogram, the vertical dashed green line indicates the period of the transits.

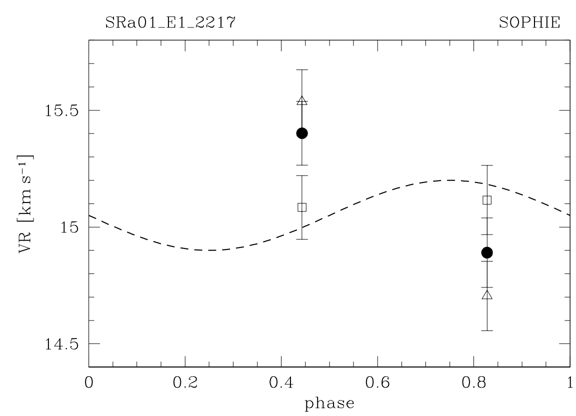

Fig. 6 Phase-folded RVs of SRa01_E1_2217 obtained with SOPHIE, computed with the F0 (open squares), G2 (dark circles) and K5 (open triangles) template respectively, indicating a diluted eclipsing binary. The dotted curve shows the signal expected for a $1\,M_\mathrm{J}$ transiting companion.

SRa01_E2_1346: This candidate shows 0.9%-deep V-shaped transits lasting 4.5 hours with a period of 2.7 days. The transit is observed to be about twice as deep in red as in blue, which – together with the long duration – led to a priority 3 classification by the detection group. However, this candidate was given priority 2 for follow-up because of its relative brightness. The lightcurve is affected by hot pixels that inhibit a a detailed analysis of out of transit variations.

This candidate was observed with SOPHIE in December 2008. No peak was detected in the CCF, indicating an early type and/or very rapidly rotating star. However the transits are V-shaped and almost twice as deep in the red channel as in the blue channel (the difference is significant at the 6σ level). This is thus most likely to be an eclipsing binary with orbital period equal to twice the photometric period.

SRa01_E1_3590: This candidate shows 1%-deep transits lasting 3.7 hours with a period of 2.8 days. The light curve is relatively noisy and hence the transit shape is not very well determined: initial analysis with a trapezoidal model found it to be V-shaped. Together with the relatively long transit duration, this led to a priority 2 classification by the detection team, and the candidate was initially excluded from follow-up because of the faint host star. More detailed modelling with a full transit model later indicated that the transit was unlikely to be grazing, and the duration had been somewhat over estimated, so the detection ranking was revised to priority 1, and the follow-up ranking to priority 2. However, no follow-up observations have yet been obtained for this candidate.

Two hour HARPS exposures was done on this target on 2011 February but no cross-correlation function could be detected indicating a early type star and/or a very rapidly rotating star.

SRa01_E2_4061: This candidate shows 3.7%-deep, U-shaped transits lasting 4.5 hours with a period of 5.8 days. All other indicators being compatible with a planetary transit, this candidate was classified as priority 1 by the detection team. It was initially excluded from the follow-up because of the faint host star, and later given a priority 3 follow-up ranking (accounting for the fairly deep transits). No follow-up observations have yet been obtained for this candidate.

SRa01_E2_1968: This candidate shows 0.7%-deep V-shaped transits lasting 2.5 hours with a period of 2.9 days. The transit shape could not be determined conclusively from the relatively noisy light curve, but is most likely V-shaped. Marginal detections of a secondary eclipse, of depth differences between odd- and even-numbered transits, and of ellipsoidal variability led to a priority 2 classification by the detection group. A slightly lower priority of 3 was adopted for the follow-up, owing to the weak but multiple indicators of binarity.

SRa01_E1_2579: This candidate shows 2.2%-deep V-shaped transits lasting 4.9 hours with a period of 5.7 days. Marginal detections of a secondary eclipse and of depth differences between odd- and even-numbered transits led to a priority 2 classification by the detection group. It was initially excluded from the follow-up because of the faint host star, and later given a priority 3 follow-up ranking (accounting for the weak but multiple indicators of binarity). No follow-up observations have yet been obtained for this candidate.

SRa01_E2_2457: This candidate shows 3%-deep V-shaped transits lasting 3.2 hours with a period of 5.3 days. Marginal detection of depth differences between odd- and even-numbered transits – together with the long duration – led to a priority 3 classification by the detection group. It was initially excluded from the follow-up because of the faint host star, and later given a priority 3 follow-up ranking (accounting for the weak but multiple indicators of binarity). No follow-up observations have yet been obtained for this candidate.

SRa01_E2_2822: This candidate shows 1.5%-deep U-shaped transits lasting 3.5 hours with a period of 2.4 days. The light curve shows some evidence for a secondary eclipse and ellipsoidal variability, which was initially deemed marginal ··· leading to a priority 3 classification by the detection group ··· but later confirmed by a more careful analysis. The final follow-up classification for this object was therefore priority 4 (indicating that no follow-up should be performed).

SRa01_E1_2618: This candidate shows 3.5%-deep U-shaped transits lasting 5.7 hours with a period of 9.5 days. The transit shape is somewhat distorted, indicating a possible false alarm (caused by discontinuities in the light curve, themselves due to charged particles hitting the detector), leading to a priority 3 classification by the detection group. A more detailed examination of individual transits later confirmed that this object was indeed a false alarm. The final follow-up classification for this object was therefore priority 4 (indicating that no follow-up should be performed).

5.2 SRa02 candidates

SRa02_E2_0628: The candidate E2_0628 has transits of 0.4% depth lasting 3.4 hours every 4.395 days and was detected during alarm mode. The transit is totally V-shaped, which is a strong indication for an eclipsing binary and deepest in blue with insignificant colour differences in the other two bands. The ingress and egress are slightly asymmetric, which might be caused by the noise in the lightcurve.

The target was observed with SOPHIE on 2008 December. The 3 radial velocity measurements do not phase with the transit ephemeris and are correlated with the bisector span (see Fig. 8) confirming a blend with a background eclipsing binary within the 3 arcsec of SOPHIE fiber acceptance.

SRa02_E2_0486: CoRoT detects 1.5% deep transits with a period of 15.14 days in E2_0486. The transits are U-shaped and show a duration of 7 hours and are deepest in blue. This candidate was detected during alarm mode. The host star is very bright ($R = 12.9$).

We obtained 4 SOPHIE measurements on 2008 December, 2009 February and November. The velocities, shown in Fig. 9, phase with the transit ephemeris assuming an eccentric orbit ($e = 0.285$) with semi-amplitude of 12.2 $\mathrm{km\,s^{-1}}$ which led to a transiting companion in the stellar mass domain with a mass ratio of 0.15. The orbital eccentricity may explain the long duration of the transit appearing in the apastron. ON-OFF photometry was performed on E2_0486 with the 1-m Wise telescope on 2009 January 6 confirming the transit. The investigation of this candidate is ongoing to clarify the nature of the secondary.

SRa02_E2_0893: The candidate E2_0893 reveals a 2.0% deep transit every 2.65 days detected during alarm mode. Two measurements were performed with SOPHIE on 2008 December and 2009 February with radial velocities separated by about 20 $\mathrm{km\,s^{-1}}$ (see in Fig. 10). Under the assumptions that the spectroscopic binary follows the CoRoT ephemeris and that the orbit is circular, it would correspond to a semi-amplitude K of about 21.08 $\mathrm{km\,s^{-1}}$ and a mass ratio of only 0.1. This companion is then probably a very low mass star near the hydrogen-burning limit. We note that this scenario explains the ellipsoidal variation visible in the CoRoT lightcurve. This was confirmed by additional spectroscopy and radial velocity measurements performed at the McDonald observatory. By co-adding two spectra from the observation, the parameters for the central star were determined. The effective temperature of the host-star $T_{\rm eff} = 7375 \pm 125 K$ and a $\log g$of 3.4 to 4.2 imply a spectral type F0 to A9 subgiant or dwarf under the assumption of solar metallicity. The precision of the values are limited by the low signal-to-noise ratio of only 15 $\cdots$ 20 at 5500 Å. Taking

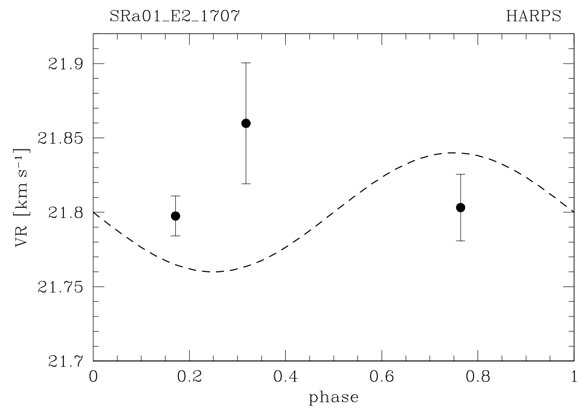

Fig. 7 Phase folded RVs of SRa01_E1_1707 obtained with HARPS. The dotted curve corresponds to the signal expected for a Saturn-mass transiting companion.

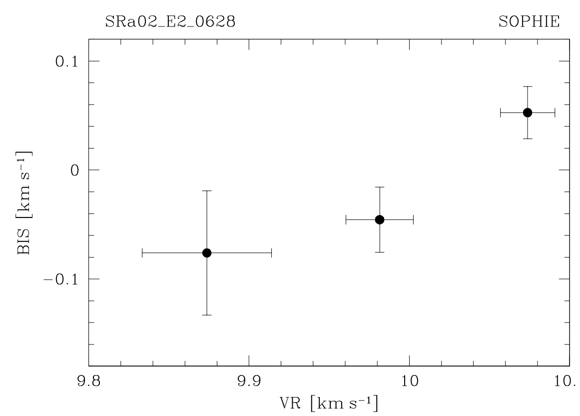

Fig. 8 Bisector span versus radial velocity of SRa02_E2_0628 showing a correlation which reveals a diluted eclipsing binary.

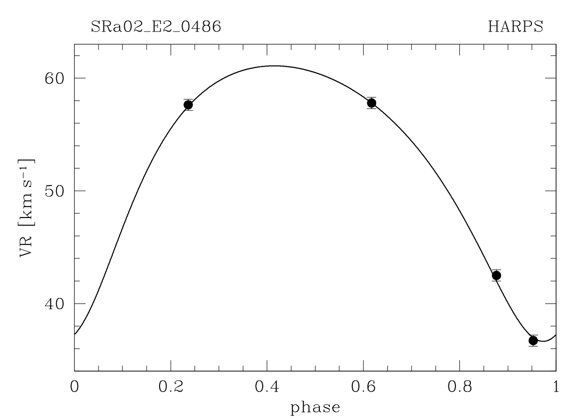

Fig. 9 Phase folded radial velocity of SRa02_E2_0486 obtained with HARPS. The curve corresponds to the best Keplerian fit using the additional constraint of the transit ephemeris and reveals a low-mass star transiting companion.

into account the uncertainty of the log $g$the mass of the primary is in the range of $1.66\ldots3.3$ $M_\odot$ and the companion would have a mass between 0.18 and 0.30 $M_\odot$, which excludes a brown dwarf.

SRa02_E2_1065: E2_1065 candidate corresponds to the longest period (22.43 days) found in this short run SRa02. The two transits present a depth of 1.3%, the first one being found in alarm mode. The transits are U-shaped and show a significant colour difference of 0.86%, with the blue transits twice as deep as the red ones.

Three measurements were done with SOPHIE on 2008 December, 2009 January and February. The strong radial velocity variations may fit the transit ephemeris is we assume an eccentric orbit, which might also explain the long transit duration. With only 3 points and 4 parameters (e, ω, K and V0), there is not an unique orbital solution. We present in Fig. 11 a solution with e=0.27 and K=10.3 $\mathrm{km\,s^{-1}}$ which led to a mass ratio of 0.14. Few additional RV measurements will allow to constraint the parameters of this system.

SRa02_E2_0749: The candidate E2_0749 shows a short period transit signal (2.5 days) with a depth of 1.85% and a transit duration of 1.880 hours. It was detected during alarm mode. The transits are slightly deeper (+0.61%) in red than in blue an very V-shaped which results in a high inclination of 80.87 deg. The lightcurve shows strong ellipsoidal variations indicating a massive companion.

The two SOPHIE measurements made in 2008 December reveal a low-mass stellar companion with a semi-amplitude K of 31.17 $\mathrm{km\,s^{-1}}$ and a mass ratio of 0.2 (see Fig. 12). This scenario is in agreement with the clear ellipsoidal variation seen in the lightcurve. The transit of E2_0749 was also observed with the 1-m Wise telescope on 2009 January 6 with duration and depth similar to the CoRoT lightcurve.

SRa02_E1_4106=CoRoT-15b: The candidate E1_4106, with a 0.743 ± 0.025% deep transit and a 3.059 day period. The tranist is very U-shaped and has a duration of 3.8 hours. This was the highest priority candidate from the detection teams and for the follow-up.

It has been established as of brown dwarf origin by HARPS and HIRES between 2009 November and 2010 February. The data are presented and discussed by Bouchy et al. (2011). CoRoT-15b has a mass of 63.3 M_{Jup} and a radius of 1.12 R_{Jup} and orbits an F7V star. Additional observations designed to acquire higher quality spectra of the star would be highly desirable to improve the size determination of the host star and the brown dwarf.

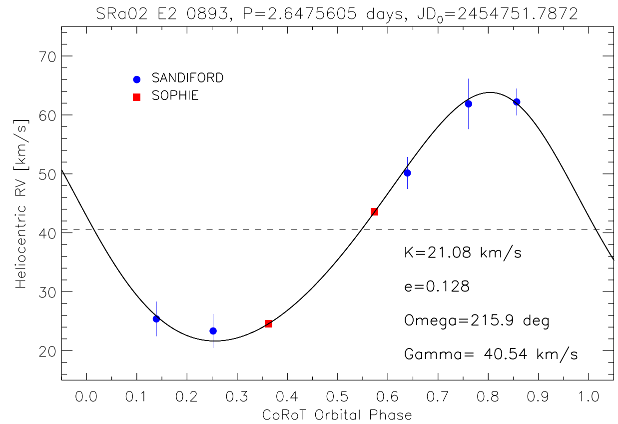

Fig. 10 Phase folded radial velocity of SRa02_E2_0893 obtained with SOPHIE (red squares) and SANDIFORD (blue circles). The curve corresponds to the eccentric orbit fit and indicates a very low-mass star transiting companion.

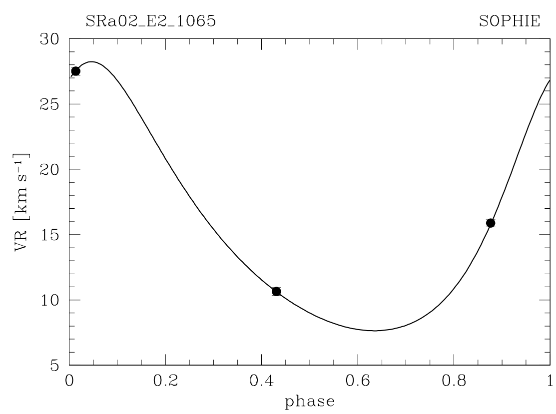

Fig. 11 Phase folded radial velocity of SRa02_E2_1065 obtained with SOPHIE. The curve corresponds to one Keplerian solution using the constraint of the transit ephemeris and indicates a low-mass star transiting companion.

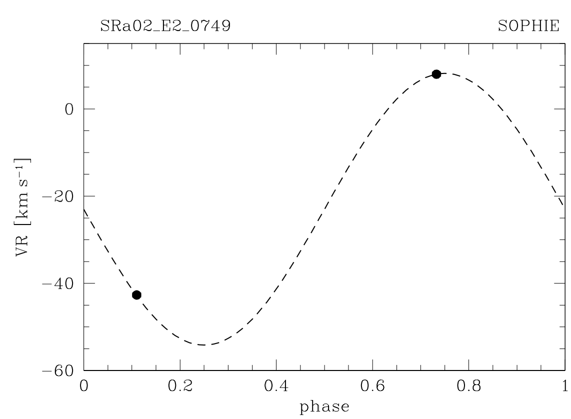

Fig. 12 Phase folded radial velocity of SRa02_E2_0749 obtained with SOPHIE. The curve corresponds to the circular orbit fit and indicates a low-mass star transiting companion.

SRa02_E1_3444: The lightcurve of this candidate shows a shallow transit (0.3%) every 1.44 days. Like E1_4106 it was a very high priority candidate from the detection teams and the follow-up team. The transit is U-shaped and has a duration of 2.2 hours. The ingress and egress are asymmetric, which is hard to determine for shallow transits. The host star is very faint ($R = 15.2$) and slightly blue ($J - K = 0.3$).

Three HARPS measurements were made on this candidate on 2010 February. The wide CCF indicates a fast rotating star and the photon noise uncertainty on the radial velocity is at the level of 400 $\mathrm{m\,s^{-1}}$. No RV variations were found on this target at this level which is not surprising considering that the expected signature of a Neptune like companion is only 10 $\mathrm{m\,s^{-1}}$. E1_3444 was observed with the CFHT on 2010 February which permit to identify that the signal is coming from a contaminant star located at 20 arcsec. This contaminant star is furthermore an other CoRoT target - SRa02_E1_2540 - which was identified as a deep eclipsing binary. Thus the shallow transit observed by CoRoT on E1_3444 is caused by this background eclipsing binary.

SRa02_E1_1978: E1_1978 presents a 0.64% deep transit with a period of 2.5156 days. The transit is U-shaped with colour differences of 0.2% deeper in red than in green. The transit duration is almost 2 hours.

Two SOPHIE measurements made in 2009 November and 2010 October show a clear correlation between the radial velocity and the bisector span indicating a blend with a background eclipsing binary (see Fig. 13). A triple system can also explain this scenario.

SRa02_E2_1011: With a depth of only 0.096%, E2_1011 is the shallowest transit of the SRa02 run. The transit with a periodicity of 1.3178 days has a duration of 1.834 ± 0.19 and is V-shaped. The transit signal was initially found in the red channel of the lightcurve only. In fact the transit signatures in blue and green are at the limit of the detection threshold.

This transiting candidate was first observed with SOPHIE. The two measurements made in 2009 November were unfortunately strongly contaminated by the diffused moon light. The two corrected radial velocity does not show variation at the level of 100 $\mathrm{m\,s^{-1}}$. Two measurements were made with HARPS on February 2011 at the expected extrema phases. No significant variation was detected at the level of 18 $\mathrm{m\,s^{-1}}$. Assuming a 1 $\mathrm{M_\odot}$ star, we can excluded at 3σ a companion with mass greater than 0.146 $\mathrm{M_{Jup}}$. However with such a shallow transit, one may expect a transiting companion with a mass smaller than Neptune and hence a RV semi-amplitude smaller than 10 $\mathrm{m\,s^{-1}}$. Such a candidate may be re-observed intensively with HARPS if the transit events are confirmed to be on the main stars and not in one of the close contaminants. The bright nearby source SRa02_E1_3249 is a pulsator and contaminates is uncertain. Investigating other possible sources for contamination we found SRa02_E1_0098, which lightcurve correlates with E2_1011.

No preparatory or follow-up imagery of this target exists; the psf of a 4mag fainter star (USNO-B1 0962-0098925) 9.3 arcsec SE of the target lies partially in the target aperture which makes it a potential source for a false positive.

SRa02_E2_4850: The 1.06% deep transit of E2_4850 was confirmed from the ground by both OGS on 2010 January and by CFHT on 2010 February. With a 2.06 days period, this hot Jupiter candidate transiting a very faint star ($m_R = 15.8$) will need significant observing time with the risk to not reach a sufficient level of accuracy in the parameter determination compared to the up-to-day known population of transiting hot Jupiter. The V-shaped signature of the transit is caused by the inclination of 70° corresponding to a high impact factor of 0.89.

SRa02_E2_4326: This faint candidate shows a transit with a depth of 0.476% every 2.887 days. With a R-magnitude of 15.6 this candidate is too faint for any radial-velocity follow up. The lightcurve is very noisy causing an asymmetric transit shape. The shallow transits inhibit a precise determination of the shape and therefore the inclination.

SRa02_E1_5401: SRa02_E1_5401 shows a transit every 1.5038 days and was observed by the IAC80 in Oct 2009 and by the 1.2m MONET telescope in Nov. 2010. Neither of these could verify the relatively deep transit of 2.2% which might be explained by an underestimate of the ephemeris error being larger than the one from the CoRoT lightcurve. The shape of the transit is slightly asymmetric showing a high level of activity in the egress. The spectral type of the host star is K6V. The lightcurve shows a possible secondary eclipse with a depth of 4.5 mmag at a 5σ level. No spectroscopic observation is carried out as long as the source of the transit is undetermined.

SRa02_E2_4852: This candidate shows 1.68%-deep V-shaped transits lasting 5.1 hours with a period of 4.817 days. The light curve shows some evidence for a secondary eclipse with a depth of 4 mmag at a 4σ detection level, ranking this candidate to a priority 3 classification by the detection group. The final follow-up classification for this object was therefore priority 3.

SRa02_E1_4680: This candidate shows 0.7%-deep V-shaped transits lasting 2.3 hours with a period of 0.57 days. The ingress and egress shapes are slightly different, which might be explained by the low signal-to-noise ratio. The light curve shows some evidence for a secondary eclipse at a 4σ level, ellipsoidal variability and minor differences between odd and even transits. As a potential binary object this candidate was ranked priority 3 by the detection group and priority 3 for final follow-up classification for this object.

SRa02_E1_4465: This candidate shows 4.45%-deep strong V-shaped transits lasting 1.960 hours with a period of 4.536 days. The host star is very faint ($R = 15.8$) and moderately blue ($J - K = 0.5$), in agreement with the spectral type of a F9 dwarf. The light curve shows some evidence for ellipsoidal variability leading to a priority 3 classification by the detection group. This fact and the object's faintness were the reason for priority 3 as a final follow-up classification for this object.

SRa02_E1_3400: This candidate shows 2.23%-deep transits lasting 4.53 hours with a period of 2.9 days. The inclination of 83.58° is derived from the fitted impact parameter of 0.55. The host star is very faint ($R = 15.0$) and moderately blue ($J - K = 0.3$), its spectral type is F4V. The light curve shows some evidence for ellipsoidal variability and there is a slight difference between odd and even transits. As a potential binary object, this candidate was given a priority 3 classification by the detection group and classified priority 3 for the follow-up.

SRa02_E2_4361: This candidate shows 4.9%-deep transits lasting 3.6 hours with a period of 13.6 days. The detection group ranked this candidate as priority 3, because of the transit depth indicating a stellar companion. The final follow-up classification for this object was priority 3 based on the faintness of the host star of 15.8 magnitudes in R-band.

SRa02_E1_5136: This candidate shows 1.27%-deep transits lasting 2.6 hours with a period of 2.009 days. The impact parameter is 0.85 implying an inclination of 78.76°. The host star is very faint ($R = 15.8$) and moderately blue ($J - K = 0.5$), in agreement with the spectral type of a F6 dwarf. The light curve shows some evidence for a secondary eclipse, differences between odd and even transits and ellipsoidal variability, which led to a priority 3 classification by the detection groups. The final follow-up classification for this object was priority 3 based on the faintness of the host star.

SRa02_E1_2903: This candidate shows 0.2%-deep V-shaped transits lasting 1.9 hours with a period of 5.6 days. The host star is very faint ($R = 15.2$) and moderatly blue ($J - K = 0.5$), which is not in agreement with the given spectral type G3V. This candidate was classified as priority 3 by the detection group due to the faintness of the star and the shallow transits. The final follow-up classification for this object was therefore priority 3.

6 Discussion / Conclusions

SRa01 was the first short observation run of CoRoT. 8 190 stars were observed in total resulting in a quite limited number of 12 relevant planetary candidates. This run was penalised by the lack of photometry follow-up. One good candidate is E1_0770 in the domain of a Saturn like object (as CoRoT-8b or HD149026b) is still pending. Two candidates could be identified as a blend, three showed no CCF, leaving four candidates that received no follow-up observation due to the faintness of the host star and one false alarm.

In SRa02 10 305 stars were observed from which 19 transiting candidates were identified, 10 of them receiving follow-up observations. The remaining 9 could not be observed due to the low magnitude (< 15) of the host stars. E1_3444 turned out to be a brown dwarf. Six candidates turned out to be eclipsing binaries including two background eclipsing binaries. One candidate could be clearly identified as a blend and a second one, E1_1011 showed no significant RV variation, which can be a possible blend.

SA, NG and AM acknowledge support from a standard grant and a studentship from the UK Science and Technology Facilities Council.

Some of the data published here were acquired with the IAC80 telescope operated by the Instituto de Astrofísica de Tenerife at the Observatorio del Teide and we thank its observing staff. The team at the IAC acknowledges support by grants ESP2007-65480-C02-02 and AYA2010-20982-C02-02 of the Spanish Ministerio de Ciencia e Inovacio ń. OT:0.8m ()

Some data was obtained at Observatoire de Haute Provence with SOPHIE and HARPS spectrograph at ESO La Silla Observatory (184.C-0639).OHP:1.93m () ESO:3.6m ()

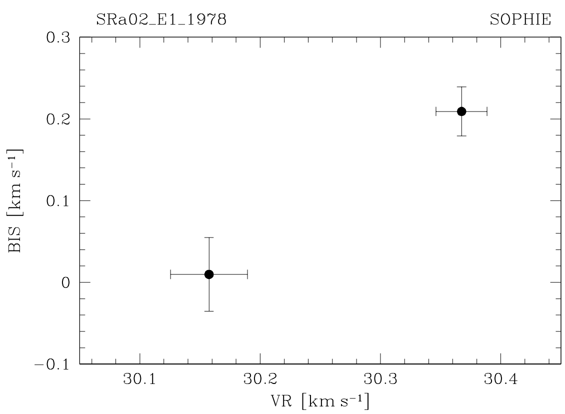

Fig. 13 Bisector span versus radial velocity of SRa02_E2_0628 showing a correlation which reveals a diluted eclipsing binary.

References

Aigrain, S., Pont, F., Fressin, F., Alapini, A., Alonso, R., Auvergne, M., Barbieri, M., Barge, P., Bordé, P., Bouchy, F., Deeg, H., de La Reza, R., Deleuil, M., Dvorak, R., Erikson, A., Fridlund, M., Gondoin, P., Guterman, P., Jorda, L., Lammer, H., Léger, A., Llebaria, A., Magain, P., Mazeh, T., Moutou, C., Ollivier, M., Pätzold, M., Queloz, D., Rauer, H., Rouan, D., Schneider, J., Wuchter, G., Zucker, S.: Astron. Astrophys. **506**, 425 (2009). 0903.1829. doi:10.1051/0004-6361/200911885

Alencar, S.H.P., Teixeira, P.S., Guimarães, M.M., McGinnis, P.T., Gameiro, J.F., Bouvier, J., Aigrain, S., Flaccomio, E., Favata, F.: A&A **519**, 88 (2010)

Auvergne, M., Bodin, P., Boisnard, L., Buey, J., Chaintreuil, S., Epstein, G., Jouret, M., Lam-Trong, T., Levacher, P., Magnan, A., Perez, R., Plasson, P., Plesseria, J., Peter, G., Steller, M., Tiphène, D., Baglin, A., Agogué, P., Appourchaux, T., Barbet, D., Beaufort, T., Bellenger, R., Berlin, R., Bernardi, P., Blouin, D., Boumier, P., Bonneau, F., Briet, R., Butler, B., Cautain, R., Chiavassa, F., Costes, V., Cuvilho, J., Cunha-Parro, V., de Oliveira Fialho, F., Decaudin, M., Defise, J., Djalal, S., Docclo, A., Drummond, R., Dupuis, O., Exil, G., Fauré, C., Gaboriaud, A., Gamet, P., Gavalda, P., Grolleau, E., Gueguen, L., Guivarc'h, V., Guterman, P., Hasiba, J., Huntzinger, G., Hustaix, H., Imbert, C., Jeanville, G., Johlander, B., Jorda, L., Journoud, P., Karioty, F., Kerjean, L., Lafond, L., Lapeyrere, V., Landiech, P., Larqué, T., Laudet, P., Le Merrer, J., Leporati, L., Leruyet, B., Levieuge, B., Llebaria, A., Martin, L., Mazy, E., Mesnager, J., Michel, J., Moalic, J., Monjoin, W., Naudet, D., Neukirchner, S., Nguyen-Kim, K., Ollivier, M., Orcesi, J., Ottacher, H., Oulali, A., Parisot, J., Perruchot, S., Piacentino, A., Pinheiro da Silva, L., Platzer, J., Pontet, B., Pradines, A., Quentin, C., Rohbeck, U., Rolland, G., Rollenhagen, F., Romagnan, R., Russ, N., Samadi, R., Schmidt, R., Schwartz, N., Sebbag, I., Smit, H., Sunter, W., Tello, M., Toulouse, P., Ulmer, B., Vandermarcq, O., Vergnault, E., Wallner, R., Waultier, G., Zanatta, P.: A&A **506**, 411 (2009)

Baglin, A., Auvergne, M., Boisnard, L., Lam-Trong, T., Barge, P., Catala, C., Deleuil, M., Michel, E., Weiss, W.: In: 36th COSPAR Scientific Assembly. COSPAR, Plenary Meeting, vol. 36, p. 3749 (2006)

Baranne, A., Queloz, D., Mayor, M., Adrianzyk, G., Knispel, G., Kohler, D., Lacroix, D., Meunier, J., Rimbaud, G., Vin, A.: A&AS **119**, 373 (1996)

Bouchy, F., Moutou, C., Queloz, D., the CoRoT Exoplanet Science Team: In: Transiting Planets. IAU Symposium, vol. 253, p. 129 (2009)

Bouchy, F., Deleuil, M., Guillot, T., Aigrain, S., Carone, L., Cochran, W.D., Almenara, J.M., Alonso, R., Auvergne, M., Baglin, A., Barge, P., Bonomo, A.S., Bordé, P., Csizmadia, S., de Bondt, K., Deeg, H.J., Díaz, R.F., Dvorak, R., Endl, M., Erikson, A., Ferraz-Mello, S., Fridlund, M., Gandolfi, D., Gazzano, J.C., Gibson, N., Gillon, M., Guenther, E., Hatzes, A., Havel, M., Hébrard, G., Jorda, L., Léger, A., Lovis, C., Llebaria, A., Lammer, H., MacQueen, P.J., Mazeh, T., Moutou, C., Ofir, A., Ollivier, M., Parviainen, H., Pätzold, M., Queloz, D., Rauer, H., Rouan, D., Santerne, A., Schneider, J., Tingley, B., Wuchterl, G.: A&A **525**, 68 (2011)

Carpano, S., Cabrera, J., Alonso, R., Barge, P., Aigrain, S., Almenara, J., Bordé, P., Bouchy, F., Carone, L., Deeg, H.J., de La Reza, R., Deleuil, M., Dvorak, R., Erikson, A., Fressin, F., Fridlund, M., Gondoin, P., Guillot, T., Hatzes, A., Jorda, L., Lammer, H., Léger, A., Llebaria, A., Magain, P., Moutou, C., Ofir, A., Ollivier, M., Janot-Pacheco, E., Pätzold, M., Pont, F., Queloz, D., Rauer, H., Régulo, C., Renner, S., Rouan, D., Samuel, B., Schneider, J., Wuchterl, G.: A&A **506**, 491 (2009)

Deeg, H.J., Gillon, M., Shporer, A., Rouan, D., Stecklum, B., Aigrain, S., Alapini, A., Almenara, J.M., Alonso, R., Barbieri, M., Bouchy, F., Eislöffel, J., Erikson, A., Fridlund, M., Eigmüller, P., Handler, G., Hatzes, A., Kabath, P., Lendl, M., Mazeh, T., Moutou, C., Queloz, D., Rauer, H., Rabus, M., Tingley, B., Titz, R.: Astron. Astrophys. **506**, 343 (2009). 0907.2653. doi:10.1051/0004-6361/200912011

Deleuil, M., Meunier, J.C., Moutou, C., Surace, C., Deeg, H.J., Barbieri, M., Debosscher, J., Almenara, J.M., Agneray, F., Granet, Y., Guterman, P., Hodgkin, S.: Astron. J. **138**, 649 (2009). doi:10.1088/0004-6256/138/2/649

Favata, F., Micela, G., Alencar, S., Aigrain, S., Zwintz, K.: Highlights of Astronomy **15**, 752 (2010)

Flaccomio, E., Micela, G., Favata, F., Alencar, S.P.H.: A&A **516**, 8 (2010)

Mandel, K., Agol, E.: ApJL **580**, 171 (2002)

Mayor, M., Pepe, F., Queloz, D., Bouchy, F., Rupprecht, G., Lo Curto, G., Avila, G., Benz, W., Bertaux, J., Bonfils, X., Dall, T., Dekker, H., Delabre, B., Eckert, W., Fleury, M., Gilliotte, A., Gojak, D., Guzman, J.C., Kohler, D., Lizon, J., Longinotti, A., Lovis, C., Megevand, D., Pasquini, L., Reyes, J., Sivan, J., Sosnowska, D., Soto, R., Udry, S., van Kesteren, A., Weber, L., Weilenmann, U.: The Messenger **114**, 20 (2003)

Moutou, C., Pont, F., Bouchy, F., Deleuil, M., Almenara, J.M., Alonso, R., Barbieri, M., Bruntt, H., Deeg, H.J., Fridlund, M., Gandolfi, D., Gillon, M., Guenther, E., Hatzes, A., Hébrard, G., Loeillet, B., Mayor, M., Mazeh, T., Queloz, D., Rabus, M., Rouan, D., Shporer, A., Udry, S., Aigrain, S., Auvergne, M., Baglin, A., Barge, P., Benz, W., Bordé, P., Carpano, S., de La Reza, R., Dvorak, R., Erikson, A., Gondoin, P., Guillot, T., Jorda, L., Kabath, P., Lammer, H., Léger, A., Llebaria, A., Lovis, C., Magain, P., Ollivier, M., Pätzold, M., Pepe, F., Rauer, H., Schneider, J., Wuchterl, G.: A&A **506**, 321 (2009)

Ofir, A., Alonso, R., Bonomo, A.S., Carone, L., Carpano, S., Samuel, B., Weingrill, J., Aigrain, S., Auvergne, M., Baglin, A., Barge, P., Borde, P., Bouchy, F., Deeg, H.J., Deleuil, M., Dvorak, R., Erikson, A., Mello, S.F., Fridlund, M., Gillon, M., Guillot, T., Hatzes, A., Jorda, L., Lammer, H., Leger, A., Llebaria, A., Moutou, C., Ollivier, M., Paetzold, M., Queloz, D., Rauer, H., Rouan, D., Schneider, J., Wuchterl, G.: 1003.0427 (2010)

Pepe, F., Mayor, M., Rupprecht, G., Avila, G., Ballester, P., Beckers, J., Benz, W., Bertaux, J., Bouchy, F., Buzzoni, B., Cavadore, C., Deiries, S., Dekker, H., Delabre, B., D'Odorico, S., Eckert, W., Fischer, J., Fleury, M., George, M., Gilliotte, A., Gojak, D., Guzman, J., Koch, F., Kohler, D., Kotzlowski, H., Lacroix, D., Le Merrer, J., Lizon, J., Lo Curto, G., Longinotti, A., Megevand, D., Pasquini, L., Petitpas, P., Pichard, M., Queloz, D., Reyes, J., Richaud, P., Sivan, J., Sosnowska, D., Soto, R., Udry, S., Ureta, E., van Kesteren, A., Weber, L., Weilenmann, U., Wicenec, A., Wieland, G., Christensen-Dalsgaard, J., Dravins, D., Hatzes, A., Kürster, M., Paresce, F., Penny, A.: The Messenger **110**, 9 (2002)

Perruchot, S., Kohler, D., Bouchy, F., Richaud, Y., Richaud, P., Moreaux, G., Merzougui, M., Sottile, R., Hill, L., Knispel, G., Regal, X., Meunier, J., Ilovaisky, S., Le Coroller, H., Gillet, D., Schmitt, J., Pepe, F., Fleury, M., Sosnowska, D., Vors, P., Mégevand, D., Blanc, P.E., Carol, C., Point, A., Laloge, A., Brunel, J.: In: Ground-based and Airborne Instrumentation for Astronomy II. Society of Photo-Optical Instrumentation Engineers (SPIE) Conference Series, vol. 7014, 2008

Sing, D.K.: A&A **510**, 21 (2010)

Sung, H., Bessell, M.S., Chun, M.: AJ **128**, 1684 (2004)

Zwintz, K., Kallinger, T., Guenther, D.B., Gruberbauer, M., Kuschnig, R., Weiss, W.W., Auvergne, M., Jorda, L., Favata, F., Matthews, J., Fischer, M.: ApJ **in press** (2011)

This manuscript was prepared with the AAS LaTeX macros v5.2.

Table 1 SRa01 transit candidates. The numbers in brackets in the 'Period' and 'Epoch' columns give the corresponding uncertainties. The columns labelled 'Sha', 'Sec', 'O/E', 'Ell' and 'Col' report the transit shape ('U' for U-shaped or clearly low impact parameter, 'V' for V-shaped or clearly grazing, and '?' for uncertain), and the presence of secondary eclipses, depth differences between odd- and even-numbered transits, ellipsoidal variation and weak ($\leq$ factor 2) depth differences between transits in the different CoRoT channel ('N' for no significant detection, '?' for detection at the 2 to 5σ level, 'Y' for detection at the $> 5\sigma$ level). The mention ' $\cdots$ ' in the 'Col' column indicates that no colour information was available.

CoRoTID	WinID	R.A. (J2000.0)	Dec. (J2000.0)	R mag	Period days	Epoch HJD	Depth %	Dur. hr	Sha U/V	Sec	O/E	Ell	Col	Status
223946365	E1_3590	99.74281	9.78470	15.3	2.82734(0.00094)	2454532.1878(0.0046)	0.9	3.2	U	N	N	N	···	No CCF
223953972	E2_2457	99.84454	7.64811	15.0	5.3471(0.0012)	2454529.6270(0.0044)	3.0	3.2	V	N	N	?	···	No FUp
223956000	E1_2217	99.87258	9.36896	14.5	2.68233(0.00034)	2454531.2719(0.0018)	2.7	2.8	V	N	?	N	···	Blend
223958585	E2_2822	99.90881	7.97390	15.2	2.37542(0.00039)	2454533.2852(0.0021)	1.5	3.5	U	Y	?	Y	···	Blend from LC
223962071	E2_1346	99.95837	8.07726	14.2	2.6975(0.0011)	2454531.6408(0.0060)	0.9	4.5	V	N	N	N	Y	No CCF
223977153	E1_0770	100.19508	9.25757	13.4	6.72114(0.00083)	2454531.2616(0.0079)	0.4	3.2	U	N	N	N	?	Planet?
223984513	E2_4061	100.31412	8.73891	15.8	5.77222(0.00056)	2454531.0902(0.0015)	3.7	4.2	U	N	N	N	···	No FUp
224002596	E2_1968	100.57840	7.96723	14.6	2.90487(0.00029)	2454531.1382(0.0016)	0.7	2.5	?	?	?	?	···	No FUp
224004253	E2_1707	100.60143	8.03162	14.7	2.39824(0.00049)	2454532.2556(0.0031)	0.4	2.3	?	N	?	N	···	Blend?
224005945	E1_2618	100.62457	9.45712	15.8	11.6900(0.0090)	2454524.684(0.010)	3.5	5.7	?	N	N	N	···	False alarm
224012284	E2_2379	100.71107	8.45597	15.0	3.59024(0.00080)	2454533.4326(0.0028)	2.2	3.8	U	?	?	N	N	No CCF
224018731	E1_2759	100.79673	9.33824	15.6	5.7131(0.0021)	2454530.9607(0.0057)	2.2	4.9	V	?	?	N	···	No FUp

Table 2 SRa02 transit candidates (same legend as Table 1).

CoRoTID	WinID	R.A. (J2000.0)	Dec. (J2000.0)	R mag	Period days	Epoch HJD	Depth %	Dur. hr	Sha U/V	Sec	O/E	Ell	Col	Status
221613770	E2_0749	95.94757	5.58905	13.1	2.17579(0.00004)	2454749.28510(0.00035)	1.8	1.9	V	?	N	Y	?	SB1
221617898	E2_4852	96.01171	5.28796	14.9	4.8156(0.0045)	2454747.764(0.018)	1.8	5.7	V	?	N	N	···	No FUp
221625053	E2_4361	96.12332	5.12378	15.8	13.6806(0.0021)	2454744.4686(0.0027)	5.5	3.9	V	N	N	N	···	No FUp
221632962	E2_1065	96.24824	5.56374	13.8	22.4270(0.0034)	2454730.7362(0.0041)	1.2	7.5	U	?	?	N	Y	SB1
221643206	E2_4850	96.40682	5.83115	15.8	2.06487(0.00075)	2454749.3599(0.0072)	1.1	4.0	V	N	N	N	···	No RV FUp
221649134	E2_0628	96.49424	5.03061	13.4	4.3952(0.0014)	2454747.7715(0.0073)	0.4	3.8	V	?	N	?	N	Blend
221650456	E1_5401	96.51457	6.21251	15.9	1.50384(0.00034)	2454750.8398(0.0044)	2.2	2.2	V	Y	N	?	···	No FUp
221656539	E2_0486	96.60683	5.27267	12.9	15.14474(0.00086)	2454747.3525(0.0011)	1.7	7.2	U	N	N	N	?	SB1
221661965	E1_1978	96.69384	7.11266	14.2	2.51560(0.00030)	2454749.3458(0.0020)	0.6	2.0	U	N	N	?	Y	BEB
221664141	E1_3444	96.72890	7.26604	15.2	1.4445(0.00045)	2454750.9045(0.00739)	0.3	2.2	U	-	-	-	-	BEB
221671889	E2_4326	96.85886	5.26825	15.6	2.8872(0.0012)	2454750.1414(0.0077)	0.4	2.2	U	N	N	?	···	No FUp
221672288	E1_2903	96.86584	7.04280	15.2	5.6255(0.0032)	2454746.167(0.012)	0.2	1.9	V	N	N	N	···	No FUp
221675115	E2_0893	96.91530	5.26602	13.2	2.64755(0.00005)	2454749.14146(0.00038)	2.3	3.5	U	N	N	Y	N	SB1
221677222	E1_3400	96.95229	7.36326	15.0	2.86115(0.00044)	2454748.9232(0.0029)	2.5	4.3	V	N	?	?	···	No FUp
221682258	E1_4680	97.04236	6.59060	15.3	0.57037(0.00010)	2454751.1061(0.0032)	0.6	2.2	V	?	?	?	···	No FUp
221686194	E1_4106	97.11591	6.18624	15.8	3.05934(0.00093)	2454750.5058(0.0056)	0.7	3.7	U	?	?	N	···	CoRoT-15b
221699621	E1_1011	97.37566	6.27519	13.8	1.31781(0.00040)	2454751.1355(0.0056)	0.1	1.9	V	N	?	?	?	No sign. RV var.
221716885	E1_5136	97.71262	6.89483	15.8	2.00904(0.00058)	2454749.6415(0.0055)	1.2	2.5	?	?	?	?	···	No FUp
221722856	E1_4465	97.83629	6.91838	15.8	4.53601(0.00016)	2454748.79039(0.00070)	4.5	2.0	V	N	N	?	···	No FUp

Table 3 SRa01 eclipsing binary candidates. Period 0.0 denotes monotransits

CoRoTID	WinID	right ascension (J2000.0)	declination (J2000.0)	J mag	K mag	period days	epoch HJD	Depth %
223923921	E1_0726	99.437939	+10.236565	11.994	11.561	0.0000	2454539.06653	0.8
223926956	E1_1781	99.480273	+09.515616	13.511	13.099	1.5737	2454534.40962	1.8
223929762	E1_1877	99.519635	+09.775863	13.509	13.002	13.9058	2454547.15958	5.4
223931925	E2_3220	99.550456	+07.988767	14.339	13.804	6.1408	2454539.31948	5.7
223935677	E2_0924	99.601761	+08.666375	12.554	12.025	0.9353	2454533.54347	2.0
223935942	E2_1088	99.605378	+08.081409	12.838	12.608	3.6333	2454533.89815	7.0
223937373	E2_0776	99.624596	+08.773969	12.272	11.856	1.0317	2454533.38410	11.2
223937598	E2_0825	99.627082	+08.756883	11.094	9.921	1.7355	2454534.24445	2.3
223939728	E1_1113	99.654200	+09.109582	12.088	11.641	11.2173	2454536.95874	23.0
223940732	E2_3999	99.666635	+08.246565	14.040	13.489	1.4064	2454533.75103	14.9
223941069	E2_4150	99.670720	+08.503760	14.572	14.015	1.4255	2454533.39340	3.6
223941278	E1_1340	99.673803	+10.219626	12.008	11.066	1.2578	2454533.88676	5.1
223941828	E2_4553	99.681243	+08.815768	11.987	11.562	2.0421	2454534.83373	7.9
223941881	E2_1456	99.682342	+08.294926	13.389	13.134	0.8855	2454533.71847	0.6
223942686	E1_0360	99.693221	+10.265366	10.802	10.194	3.8247	2454535.36652	7.8
223943482	E1_2754	99.703798	+09.832825	13.814	13.248	2.2467	2454534.87135	10.2
223944492	E1_2613	99.717376	+09.806249	13.600	13.013	0.8471	2454533.70382	1.3
223944684	E1_0944	99.719652	+09.775457	12.999	12.657	2.2773	2454533.60932	0.6
223945037	E1_3325	99.724498	+09.375216	14.321	13.647	6.2368	2454533.95056	2.7
223945374	E2_1062	99.729248	+07.739816	12.856	12.373	0.8953	2454534.15100	7.3
223945778	E2_1169	99.735421	+08.328819	13.720	13.227	2.8550	2454534.50511	1.0
223946171	E1_0393	99.740261	+09.935358	11.533	11.218	7.7132	2454536.38657	7.5
223946242	E1_2416	99.741396	+09.665241	13.191	12.375	1.2801	2454533.38862	11.4
223947472	E2_2629	99.756834	+07.773057	13.740	13.443	2.0261	2454535.27857	1.1
223947647	E1_1280	99.759345	+10.250665	12.668	12.213	1.4458	2454533.62531	0.4
223948253	E1_3347	99.767199	+09.787673	14.442	13.881	0.9216	2454534.13342	1.8
223948645	E2_2258	99.772409	+08.875686	13.782	13.159	2.3555	2454534.39714	1.1
223949716	E2_0718	99.786730	+08.514941	11.820	11.440	3.9182	2454535.30319	45.3
223950353	E2_3609	99.795236	+08.568054	14.088	13.555	1.0506	2454533.55604	17.0
223951052	E2_0291	99.804414	+07.936279	12.000	11.766	11.8082	2454535.07380	1.7
223951589	E1_2103	99.811720	+09.575235	14.098	13.796	7.3336	2454538.63988	5.4
223953972	E2_2457	99.844536	+07.647904	14.679	14.416	5.3560	2454534.95420	2.0
223954720	E1_2677	99.854849	+09.543918	13.728	13.239	2.8257	2454535.88574	16.6
223955448	E2_3449	99.865202	+07.874002	13.897	13.401	12.7107	2454534.28623	29.1
223955882	E1_1021	99.871303	+09.710732	12.992	12.237	1.0211	2454533.93664	15.3
223956278	E2_3734	99.876722	+08.600704	13.884	13.315	1.0803	2454533.76582	6.4
223956532	E2_0389	99.880363	+08.165193	11.680	11.275	1.4427	2454533.39325	20.8
223956789	E2_2995	99.884098	+08.567060	13.630	13.161	0.8130	2454533.70940	26.2
223956963	E1_1600	99.886528	+09.070493	13.018	11.743	13.0875	2454543.78438	6.9
223957597	E2_3238	99.895394	+08.495312	13.992	13.599	12.2442	2454538.78849	4.1
223958206	E2_0126	99.904138	+08.391648	10.662	10.581	1.0911	2454533.91404	3.1
223958210	E1_0187	99.903850	+09.263092	11.009	10.305	11.1216	2454539.33320	22.4
223958323	E2_2890	99.905696	+07.739878	14.109	13.861	2.6275	2454534.23125	35.9
223959623	E2_3829	99.922699	+08.844955	14.018	13.447	1.2497	2454534.18128	12.7
223960745	E2_3263	99.939191	+08.752823	12.874	11.834	1.3154	2454534.12405	9.2

Table 3—Continued

CoRoTID	WinID	right ascension (J2000.0)	declination (J2000.0)	J mag	K mag	period days	epoch HJD	Depth %
223962863	E2_2383	99.970196	+08.659643	13.427	13.043	0.9749	2454533.87052	4.4
223963003	E2_0915	99.972296	+08.418068	12.039	11.440	7.8846	2454538.89514	38.6
223963114	E2_4571	99.974003	+08.421585	13.338	12.397	7.8935	2454538.88570	11.0
223963205	E2_2430	99.974918	+08.085771	14.015	13.772	1.5946	2454533.62738	1.9
223964763	E1_0942	99.998533	+09.586338	12.852	11.972	11.7088	2454544.19038	18.9
223966050	E2_1471	100.017650	+07.758658	12.358	11.648	12.2442	2454545.44157	5.5
223966330	E2_3433	100.021532	+08.265016	13.962	13.682	8.6071	2454534.61249	6.8
223966541	E1_0254	100.024579	+10.181335	10.536	10.209	14.0516	2454540.32093	19.7
223971548	E1_0824	100.101832	+09.327463	12.593	11.808	3.9137	2454533.70319	41.3
223971849	E2_4407	100.106800	+07.882738	14.612	14.101	12.1327	2454540.06865	12.4
223972894	E2_3934	100.123474	+08.522076	14.375	13.935	6.8044	2454538.78321	27.7
223973671	E2_2338	100.136550	+08.339511	13.622	13.274	5.4883	2454538.65728	7.0
223974019	E2_0227	100.142005	+08.577719	11.771	11.626	16.6508	2454549.68950	38.5
223974688	E2_4052	100.153088	+08.617470	14.732	14.258	1.4633	2454533.85750	7.2
223975234	E2_1825	100.162242	+08.342917	13.256	12.874	5.9809	2454534.90496	17.3
223976178	E1_1632	100.178120	+10.297546	12.791	12.250	6.6036	2454533.61765	23.0
223979111	E2_0779	100.226609	+07.872157	11.817	11.438	0.8235	2454533.91855	4.7
223979687	E1_3334	100.236018	+09.127923	13.376	12.438	6.6402	2454537.39253	6.2
223980235	E2_4092	100.244558	+08.284349	14.232	13.691	2.0261	2454533.65718	9.7
223982103	E2_2516	100.275037	+08.029663	13.165	12.832	1.2438	2454533.69541	12.3
223982297	E2_2168	100.278459	+08.914482	12.758	12.084	1.1294	2454534.41185	7.7
223984155	E2_2021	100.308853	+08.602862	13.360	13.053	1.3838	2454533.49189	6.5
223984461	E2_3172	100.313361	+08.612929	13.854	13.429	2.9042	2454533.42125	1.6
223986812	E2_3616	100.351098	+08.038252	13.934	13.456	2.1342	2454533.36992	14.8
223992193	E1_1039	100.434277	+09.417340	13.329	12.331	3.8676	2454536.77807	24.7
223993566	E1_0802	100.454869	+10.122078	11.596	10.994	1.1822	2454533.82720	3.6
223993696	E2_3854	100.456283	+08.723048	14.038	13.512	9.5989	2454534.48759	3.6
223993744	E2_2020	100.456851	+07.994453	13.505	13.169	6.6654	2454536.08291	12.2
223994191	E1_3602	100.462870	+09.179623	14.141	13.351	3.8343	2454535.50163	12.7
223998299	E2_3973	100.520486	+08.746130	13.767	13.163	14.6697	2454540.10004	2.5
223998341	E1_1572	100.520972	+09.089563	12.649	12.002	2.8762	2454535.09606	6.5
223999491	E2_0162	100.536397	+07.711919	11.640	11.517	1.5906	2454534.29191	8.8
223999763	E2_3823	100.540288	+08.459287	14.233	13.718	2.4735	2454533.74963	5.3
224000346	E2_1370	100.548202	+07.918493	13.041	12.715	13.7611	2454536.11259	4.9
224001237	E1_1959	100.559803	+10.102330	13.625	13.129	3.0679	2454535.76084	12.4
224003482	E2_0461	100.590321	+07.741018	11.682	11.320	1.1915	2454533.46867	0.2
224004282	E2_4323	100.602224	+08.755734	14.074	13.307	4.7594	2454534.42773	10.2
224005111	E2_0224	100.613159	+08.273859	11.180	10.886	2.3411	2454535.15592	2.6
224005929	E2_1548	100.624220	+08.613081	12.633	12.145	1.1695	2454533.44685	19.1
224007535	E1_3190	100.646299	+09.932430	14.579	13.951	0.8890	2454533.64547	12.5
224007715	E2_3104	100.648516	+08.414224	13.612	13.098	14.2009	2454538.74078	20.8
224009183	E1_1408	100.668195	+10.121798	13.076	12.794	3.5779	2454536.75218	18.8
224013042	E1_0445	100.720943	+09.904484	12.596	12.252	1.5154	2454534.11677	3.1
224015696	E1_0517	100.756278	+09.325040	12.022	11.631	13.2175	2454546.50848	2.7
224016908	E2_4380	100.772724	+07.937246	14.317	13.805	13.6205	2454546.91031	11.6

Table 3—Continued

CoRoTID	WinID	right ascension (J2000.0)	declination (J2000.0)	J mag	K mag	period days	epoch HJD	Depth %
224017268	E2_4149	100.777409	+07.712875	14.324	13.754	2.0588	2454534.60406	6.7
224017753	E2_2601	100.783954	+08.954572	12.973	12.311	2.1162	2454534.87337	13.2
224022502	E2_4165	100.846337	+08.121675	14.104	13.357	14.8331	2454536.89208	25.6
500007008	E1_2986	100.155218	+09.791592	8.409	7.495	1.8535	2454533.97652	3.5
500007022	E1_0091	100.304329	+09.458864	10.296	9.905	5.2134	2454535.67181	2.9
500007038	E1_1379	100.152811	+09.789592	9.647	8.593	4.1191	2454535.57111	0.4

Table 4 SRa02 eclipsing binary candidates. Period 0.0 denotes monotransits

CoRoTID	WinID	right ascension (J2000.0)	declination (J2000.0)	J mag	K mag	period days	epoch HJD	Depth %
221604723	E2_0938	95.803912	5.354606	13.280	12.948	2.3052	2454752.20655	6.9
221613770	E2_0749	95.947567	5.589050	12.333	12.017	2.1748	2454751.46581	1.7
221614718	E2_1556	95.961912	5.230820	13.153	12.664	5.6889	2454756.61544	22.3
221616609	E2_4064	95.991820	5.539970	14.395	13.750	0.0000	2454751.47174	0.2
221617602	E2_0596	96.007300	5.246456	11.853	11.521	6.6667	2454757.21989	65.5
221620551	E2_3413	96.053814	5.160009	14.266	14.064	3.1585	2454753.47470	14.1
221621994	E2_2858	96.076303	5.665720	14.343	14.114	1.3156	2454751.73840	2.7
221625883	E2_0467	96.136306	5.082931	12.000	11.632	1.5763	2454751.27026	0.9
221630265	E2_2222	96.205809	6.171287	13.044	12.640	15.5615	2454760.99470	4.9
221630363	E2_0272	96.207370	6.100906	11.317	11.037	6.0385	2454753.77692	42.4
221631316	E2_3423	96.222356	4.963592	14.545	14.199	3.1822	2454751.88063	28.5
221632993	E2_3741	96.248906	4.830356	14.239	13.748	0.8119	2454751.34137	33.3
221633267	E2_2972	96.252870	4.836042	12.902	12.071	8.1244	2454756.21248	0.9
221634836	E2_2372	96.277148	6.109628	13.800	13.251	1.9911	2454751.11618	4.0
221638409	E2_4008	96.332370	5.473639	14.684	14.267	0.7170	2454751.67322	3.0
221638835	E2_2035	96.338653	5.103673	13.454	13.045	15.0637	2454760.09989	6.1
221638842	E1_2425	96.338762	6.612339	13.433	13.024	3.4607	2454752.26581	9.2
221639829	E1_4755	96.354775	6.270700	14.561	14.066	15.3244	2454751.93396	10.5
221639870	E1_3019	96.355514	6.365762	13.507	12.948	6.1748	2454754.57692	10.3
221640500	E2_1292	96.365592	5.370667	12.486	12.223	6.3644	2454754.09692	9.3
221641502	E1_2637	96.381167	6.722056	14.056	13.687	1.0193	2454751.68507	4.8
221641562	E2_4625	96.381975	5.155678	14.703	14.207	2.8207	2454751.46581	21.0
221644003	E1_0638	96.418481	6.558756	12.265	12.090	1.8015	2454752.59174	20.5
221646787	E2_0326	96.459612	5.761406	11.628	11.451	3.2770	2454753.21396	24.2
221648754	E1_3511	96.488481	6.799956	13.805	13.235	7.0281	2454756.73989	4.0
221649057	E1_1989	96.492962	6.280320	13.362	13.056	11.5793	2454751.68507	13.4
221649991	E2_2456	96.507173	4.925564	14.237	13.720	0.8948	2454751.92803	6.7
221650319	E1_1028	96.512387	6.986570	12.660	12.466	2.2044	2454752.22433	11.7
221650584	E2_4397	96.516623	5.333850	14.544	14.048	1.9556	2454751.50729	5.0
221652902	E2_1697	96.552223	4.940339	12.810	12.287	0.5215	2454751.57248	0.6
221653759	E2_3755	96.565145	5.778706	13.917	13.420	2.5481	2454751.52507	33.3
221654221	E2_4187	96.572084	5.989073	14.334	13.823	5.2978	2454755.36507	25.6
221655934	E2_0127	96.597650	5.196620	11.042	10.876	11.5141	2454757.87174	2.3
221656539	E2_0486	96.606825	5.272670	11.622	11.222	15.1467	2454762.49989	1.8
221657201	E1_0860	96.617481	6.877350	12.855	12.663	1.4815	2454752.27766	1.1
221658242	E1_3532	96.634345	6.621595	13.782	13.303	10.0741	2454758.26285	27.5
221658260	E1_2042	96.634778	6.782237	13.421	13.017	1.6770	2454751.90433	6.0
221658472	E1_5484	96.637698	7.097706	14.387	14.054	9.1319	2454752.87618	4.2
221658715	E1_4518	96.641381	6.436173	14.165	13.687	0.9422	2454752.02877	0.4
221661707	E1_2494	96.689984	6.159034	14.120	13.808	2.1096	2454753.10137	7.9
221662783	E2_2137	96.706845	5.462723	12.299	11.203	0.0000	2454751.13396	0.1
221663011	E1_1353	96.710948	7.205987	12.973	12.530	10.5541	2454759.00359	25.6
221663848	E1_2540	96.723981	7.269078	13.770	13.350	1.4459	2454752.33100	35.6
221664419	E2_2069	96.734131	5.153028	12.859	12.356	1.2741	2454751.47174	41.4
221664856	E2_2019	96.740773	4.952362	12.394	11.535	14.4770	2454757.67026	9.5

Table 4—Continued

CoRoTID	WinID	right ascension (J2000.0)	declination (J2000.0)	J mag	K mag	period days	epoch HJD	Depth %
221665163	E2_3433	96.745325	5.908825	14.103	13.784	3.8459	2454751.33544	13.9
221665390	E2_4671	96.749062	4.937575	14.544	13.506	2.4474	2454751.40063	32.1
221666127	E1_4649	96.760973	6.571642	14.125	13.542	11.0519	2454754.20359	7.6
221668255	E2_2435	96.797420	5.658575	13.900	13.274	0.8652	2454751.54877	15.6
221668809	E1_4910	96.806792	6.104748	14.087	13.938	0.7230	2454751.79766	1.6
221671608	E2_2294	96.854342	5.832670	13.309	12.816	7.0104	2454753.92507	10.8
221673069	E1_2089	96.880206	6.525839	13.484	13.087	5.9319	2454752.04063	37.7
221673572	E1_5447	96.888662	6.040198	13.603	13.131	14.6726	2454756.04063	7.9
221674549	E2_2775	96.905423	5.318670	13.369	12.740	12.9422	2454752.00507	7.2
221674977	E1_5517	96.912737	7.152837	14.589	14.158	0.9422	2454751.38285	6.5
221675083	E1_5061	96.914548	6.612731	14.432	13.961	7.2474	2454757.73544	8.1
221675115	E2_0893	96.915298	5.266023	12.615	12.425	2.6489	2454751.76803	2.4
221677174	E1_4719	96.951334	6.288725	14.029	13.583	2.0681	2454752.59766	20.7
221680104	E1_1708	97.003287	6.449381	12.862	12.456	15.4015	2454759.02729	6.3
221680124	E1_3773	97.003614	6.755114	14.061	13.626	2.1096	2454752.07026	7.3
221681035	E1_2338	97.020214	6.589075	13.529	13.046	0.5452	2454751.29989	20.9
221681494	E1_4606	97.029198	7.306550	14.003	13.537	1.8844	2454752.66285	2.2
221681609	E1_5241	97.030987	7.079462	14.199	13.647	0.6519	2454751.33544	7.1
221683159	E1_0192	97.058920	6.126248	9.728	8.878	29.0810	2454751.53692	34.0
221685038	E2_0131	97.094675	5.215875	10.533	10.220	4.1778	2454754.25692	76.8
221686786	E1_2677	97.127164	6.928748	13.922	13.250	0.7348	2454751.76803	3.5
221687871	E1_3227	97.147509	6.644120	12.529	11.576	0.9956	2454751.90433	0.3
221689571	E1_1395	97.181050	6.662462	12.724	12.392	1.9437	2454751.41248	2.4
221692716	E1_0359	97.240123	6.799370	11.382	11.005	7.0104	2454752.52063	8.8
221693674	E1_3588	97.259398	5.959087	12.629	11.530	14.8859	2454757.09544	3.6
221697417	E1_4022	97.332934	6.853070	14.254	13.865	15.7867	2454755.72655	7.5
221699752	E1_2384	97.378023	5.917495	13.286	12.672	11.4667	2454751.64359	2.0
221699985	E1_1835	97.382523	6.878042	13.175	12.787	5.1437	2454751.85100	37.7
221702600	E1_1444	97.431937	6.656681	12.951	12.613	5.8252	2454754.63618	9.2
221703104	E1_4677	97.441742	6.501087	13.913	13.306	13.6119	2454764.46729	8.2
221703353	E1_5254	97.446795	6.695225	14.567	14.224	0.5748	2454751.22285	20.9
221704769	E1_0461	97.474284	6.055309	11.086	10.609	5.0133	2454755.22285	80.1
221707281	E1_1244	97.521645	6.222806	11.784	10.902	2.1807	2454752.02285	38.7
221709981	E1_4841	97.572509	6.432184	13.689	12.945	11.6089	2454759.34137	9.0
221711233	E1_0961	97.596170	6.960789	12.808	12.621	9.1022	2454753.61100	3.6
221712632	E1_3162	97.623542	6.503184	13.625	13.157	13.1141	2454755.76211	5.1
221712689	E1_2305	97.624684	6.927673	13.191	12.845	8.7704	2454751.84507	4.6
221713272	E1_2485	97.637209	6.748714	13.396	12.753	1.5467	2454751.82137	30.2
221718496	E1_2137	97.746778	7.027739	13.527	13.283	5.9022	2454755.56063	12.4
221722856	E1_4465	97.836287	6.918375	14.318	13.847	4.5333	2454753.32655	4.3